

# Double-P: Hierarchical Top-P Sparse Attention for Long-Context LLMs

Wentao Ni<sup>1</sup> Kangqi Zhang<sup>2</sup> Zhongming Yu<sup>1</sup> Oren Nelson<sup>1</sup> Mingu Lee<sup>3</sup> Hong Cai<sup>3</sup> Fatih Porikli<sup>3</sup>  
Jongryool Kim<sup>4</sup> Zhijian Liu<sup>1,5</sup> Jishen Zhao<sup>1</sup>

## Abstract

As long-context inference becomes central to large language models (LLMs), attention over growing key-value caches emerges as a dominant decoding bottleneck, motivating sparse attention for scalable inference. Fixed-budget top-k sparse attention cannot adapt to heterogeneous attention distributions across heads and layers, whereas top-p sparse attention directly preserves attention mass and provides stronger accuracy guarantees. Existing top-p methods, however, fail to jointly optimize top-p accuracy, selection overhead, and sparse attention cost, which limits their overall efficiency. We present **Double-P**, a hierarchical sparse attention framework that optimizes all three stages. Double-P first performs coarse-grained top-p estimation at the cluster level using size-weighted centroids, then adaptively refines computation through a second top-p stage that allocates token-level attention only when needed. Across long-context benchmarks, Double-P consistently achieves near-zero accuracy drop, reducing attention computation overhead by up to 1.8 $\times$  and delivers up to 1.3 $\times$  end-to-end decoding speedup over state-of-the-art fixed-budget sparse attention methods.

## 1. Introduction

Recent large language models (LLMs) support increasingly long context inference, enabling applications such as retrieval-augmented generation (Fan et al., 2024; Jin et al., 2024), document understanding (Appalaraju et al., 2021; Luo et al., 2024), and long-horizon reasoning over tens or even hundreds of thousands of tokens (Grattafiori

<sup>1</sup>Department of Computer Science and Engineering, University of California San Diego, La Jolla, United States <sup>2</sup>Department of Electrical Engineering and Computer Science, University of Michigan, Ann Arbor, United States <sup>3</sup>Qualcomm AI Research, San Diego, United States <sup>4</sup>SK hynix America, San Jose, United States <sup>5</sup>NVIDIA, Santa Clara, United States. Correspondence to: Jishen Zhao <jzhao@ucsd.edu>.

Preprint. February 6, 2026.

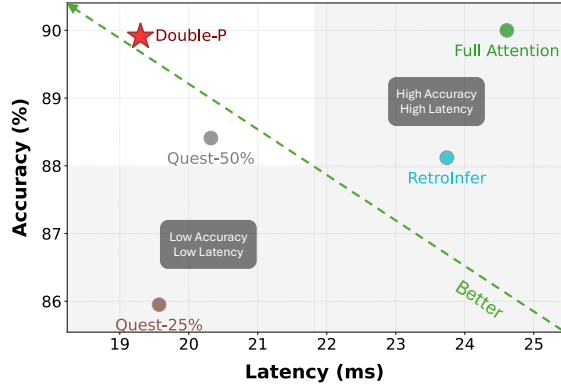
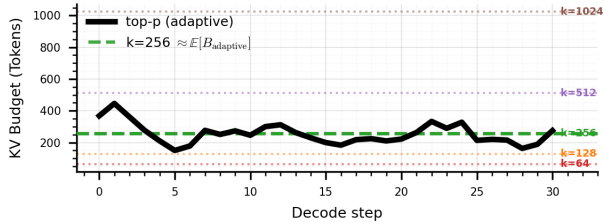


Figure 1. Average accuracy and decode latency of different sparse attention methods tested on Ruler (Hsieh et al., 2024) 32k context length. Double-P dominates existing approaches, forming a Pareto frontier that demonstrates superior efficiency–accuracy balance.

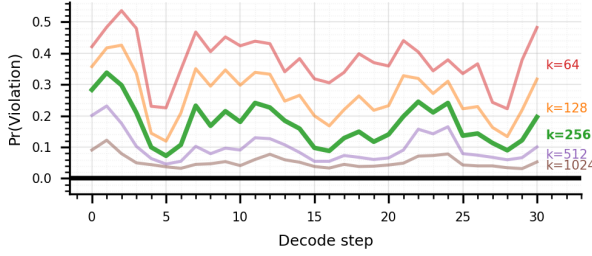
et al., 2024; Yang et al., 2025b; Team et al., 2023). While extended context improves modeling capacity, it also introduces substantial computational and memory overhead during autoregressive decoding due to attention mechanism. In practice, the attention computation dominates the bottleneck in long-context inference, calling for more efficient attention mechanisms.

Sparse attention addresses this bottleneck by restricting attention computation to a subset of tokens that are estimated to be most relevant to the current query. Most existing methods (Tang et al., 2024b; Liu et al., 2024; Zhang et al., 2025a; Liu et al., 2025b; Chen et al., 2025) adopt a *top-k* formulation, where a fixed number of tokens are selected under a predefined budget.

While simple, fixed-budget designs assume that a single budget suffices across heads, layers, and decoding steps. In practice, attention distributions vary substantially, leading to severe budget imbalance: a budget that is adequate for some heads may be overly conservative for others while remaining insufficient for more diffuse cases. Figure 2a shows that the token budget required to maintain a fixed attention mass varies significantly across decoding steps. Figure 2b further shows that enforcing any fixed budget, even the expected mean budget ( $k = 256$ ), results in non-trivial violations of the target mass ( $p = 0.95$ ) across layers. These results indicate that no single fixed budget can reli-



(a) Adaptive vs. fixed token budgets. The black curve shows the adaptive token budget required to maintain an attention mass of  $p = 0.95$  at each decoding step (averaged over heads and layers), while horizontal lines denote fixed  $k$  budgets that fail to adapt to step-wise variations in attention distribution.



(b) Violation rates across sparse attention budgets (NIAH 8K). We report the fraction of attention heads violating the target mass ( $p = 0.95$ ) during decoding. Adaptive top-p incurs zero violations, while fixed- $k$  strategies fail frequently. The expected mean budget  $k = 256$  even violates the constraint in over 20% of heads, indicating that no single fixed budget reliably satisfies top-p requirements.

Figure 2. Limitations of fixed token budgets for sparse attention.

Table 1. Comparison of Top- $p$  accuracy and cost across methods.

Method	Top- $p$		Sparse Attention Cost
	Accuracy	Cost	
Token Top-p	Medium	High	Low
Cluster	$\times$	$\times$	Medium
<b>Double-P (Ours)</b>	High	Low	Low

ably satisfy top- $p$  constraints, motivating adaptive budget allocation and highlighting the inherent limitations of top- $k$  sparse attention.

Top- $p$  sparse attention addresses this issue by constraining preserved attention mass rather than token count, retaining the minimal set of tokens whose cumulative attention exceeds a target threshold. As shown in Figure 2, top- $p$  adapts the compute budget and achieves near-zero violations. In practice, top- $p$  sparse attention comprises two stages: (1) top- $p$  estimation to identify tokens preserving a target attention mass, and (2) sparse attention computation over the selected subset. Efficient deployment therefore requires jointly optimizing estimation accuracy, selection overhead, and sparse attention cost. (Table 1).

Prior work shows that efficiently supporting top- $p$  sparse attention is challenging. Token-level approaches (Lin et al.,

2025) rely on fixed token budgets for top- $p$  estimation, which cannot reliably recover a target attention mass due to variability across heads and layers, forcing conservative budget choices. Moreover, token-level estimation incurs high selection overhead that scales linearly with context length, limiting end-to-end efficiency even with aggressive pruning.

In contrast, cluster-based sparse attention methods (Chen et al., 2025) reduce sparse attention cost by operating on cluster-level representations, but both cluster selection and sparse attention computation still rely on fixed budgets, effectively reverting to top- $k$  behavior. Consequently, these methods lack explicit control over preserved attention mass and cannot provide top- $p$  accuracy guarantees.

To address these challenges, we propose **Double-P**, a **hierarchical top-p sparse attention framework** that reduces both top- $p$  estimation and sparse attention cost while preserving attention mass guarantees. Double-P first performs **cluster-level Top-p attention score estimation** using size-weighted centroids, and then applies a **second-stage adaptive token budget allocation** to adaptively determine which clusters require exact token-level attention. Sparse attention is computed by combining exact attention over high-impact tokens with centroid-based approximations for the remainder. We further introduce **GPU efficient kernels** that minimize top- $p$  selection overhead and maximize data locality for sparse attention computation. Extensive evaluation shows that Double-P achieves up to **2.27 $\times$**  self-attention speedup and **1.26 $\times$**  end-to-end decoding speedup, forming a **superior accuracy-efficiency Pareto frontier** over existing token-level and cluster-based methods (Figure 1).

## 2. Background

### 2.1. LLM and Attention Mechanism

Large Language Models (LLMs) are built upon the Transformer architecture (Yang et al., 2025a; Liu et al., 2025a; Grattafiori et al., 2024; Team et al., 2023), where the core computational primitive is the Scaled Dot-Product Attention (Vaswani et al., 2017). In autoregressive inference, generation proceeds in two stages: a prefill stage, which processes the input prompt in parallel to construct the key-value (KV) cache, and a decoding stage, where tokens are generated sequentially using the cached representations (Kwon et al., 2023). During decoding stage, each output token is generated by attending over all previously seen tokens stored in the key-value (KV) cache (Kwon et al., 2023). Given a query token vector  $q \in \mathbb{R}^d$  at a decoding step and the cached key and value matrices  $K, V \in \mathbb{R}^{N \times d}$ , where  $d$  is the head dimension and  $N$  is the current context length, the

attention output  $o$  is computed as:

$$o = \text{Softmax} \left( \frac{\mathbf{qK}^\top}{\sqrt{d}} \right) V = \sum_{i=1}^N A_i v_i \quad (1)$$

where  $A_i$  represents the attention weight for the  $i$ -th token. In the context of long-context inference,  $N$  (the sequence length) can reach hundreds of thousands. Since the computational complexity and memory bandwidth requirements scale quadratically with  $N$ , the full attention mechanism becomes the primary latency bottleneck.

## 2.2. Sparse Attention

To reduce the overhead of full attention, sparse attention methods approximate the output by identifying and attending only to the most critical subset of tokens, i.e., those with high attention weights  $A_i$ .

**Static Selection and Permanent Eviction.** Static selection methods (Li et al., 2024) rely on predefined sparse attention structures, whereas permanent eviction methods (Xiao et al., 2023; Zhang et al., 2023) reduce attention cost by permanently removing tokens deemed unimportant during long-context processing.

**Retrieval-Based Methods.** Retrieval-based sparse attention methods aim to identify a subset of relevant tokens before computing exact attention. Existing approaches adopt different retrieval granularities, including page-level retrieval using coarse token statistics (Tang et al., 2024b; Xiao et al., 2024; Yang et al., 2025c), cluster-level retrieval via centroid-based similarity estimation (Liu et al., 2025b; Chen et al., 2025; Zhu et al., 2025; Liu et al., 2025d), and token-level approximate nearest neighbor search using structures such as product quantization, locality-sensitive hashing, or graph-based indices (Liu et al., 2024; Zhang et al., 2025a; Chen et al., 2024). While these methods significantly reduce attention cost, their retrieval quality is often sensitive to approximation error and fixed selection budgets.

**Prefill Acceleration.** Prefill acceleration methods (Jiang et al., 2024; Gao et al., 2024; Zhang et al., 2025b; Xu et al., 2025; Jones et al., 2026) focus on reducing the cost of prompt processing by exploiting sparsity in attention computation.

**Trainable Sparse Attention.** Several works (Yuan et al., 2025; Lu et al., 2025; Liu et al., 2025a) explore trainable sparse attention by learning content-based routing or token selection mechanisms.

**Top-P Sparse Attention.** Recent work (Lin et al., 2025) extends sparse attention from fixed top- $k$  to probability-based top- $p$  selection, adaptively retaining tokens whose cumulative attention mass exceeds a target threshold.

## 2.3. Other Inference Optimizations

**Layer-wise and head-wise budget allocation.** These methods (Feng et al., 2024; Tang et al., 2024a; Xiao et al., 2024) allocate KV cache budgets unevenly across layers or attention heads based on their estimated importance, reducing memory and computation while preserving model quality.

**Quantization.** Prior work (Frantar et al., 2022; Lin et al., 2024; Tseng et al., 2024; Van Baalen et al., 2024; Liu et al., 2025c) investigates low-precision quantization for large language models to reduce memory footprint and inference cost. In addition to weight quantization, recent methods (Hooper et al., 2024; Yue et al., 2024; Kang et al., 2024) further compress the KV cache using reduced precision, achieving substantial memory savings with minimal accuracy degradation.

**Linear Attention.** Linear attention methods (Katharopoulos et al., 2020; Gu & Dao, 2024) replace softmax attention with kernelized or state-space formulations to achieve linear-time sequence processing and eliminate explicit KV cache storage.

## 3. Motivation

Top-p sparse attention offers an appealing alternative to fixed-budget top- $k$  methods by directly constraining preserved attention mass and providing explicit accuracy guarantees. However, realizing these benefits efficiently in practice remains challenging.

To overcome the limitations of fixed top- $k$  budget algorithms, recent work such as Twilight (Lin et al., 2025) introduces probability-based top- $p$  sparse attention, which adaptively retains a variable number of tokens whose cumulative attention mass exceeds a target threshold  $p$ . Since exact top- $p$  selection requires computing and sorting attention scores over all tokens, Twilight adopts a *select-then-prune* pipeline that relies on approximate token-level attention estimation to identify a candidate set, applies top-p pruning on the estimated scores, and computes exact attention only on the retained tokens.

However, token-level top-p methods reveal two fundamental limitations. First, top-p estimation is typically performed under a fixed token budget, which cannot reliably recover a target attention mass due to substantial variation in attention distributions across heads, layers, and decoding steps.

Figure 3 provides empirical evidence that fixed-budget token-level top-p estimation is fundamentally unreliable. Each point represents a LongBench sample, plotting the recovered attention mass against the token budget normalized by context length. Under the commonly recommended fixed budget (e.g., 8192 tokens for Quest), 91.9% of samples fail to reach the target attention mass  $p = 0.95$ . Moreover,

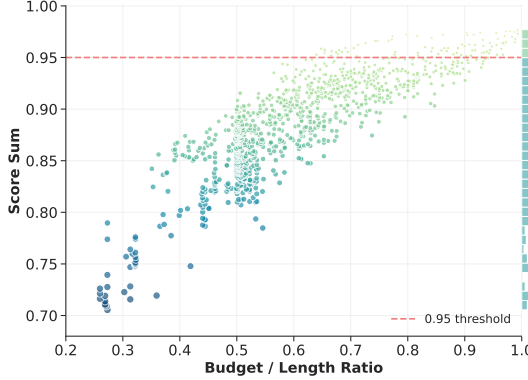


Figure 3. Failure of fixed-budget token-level Top-P estimation. Each point shows the recovered attention mass and its budget ratio for an individual LongBench sample. Under the recommended fixed budget, 91.9% of samples fail to recover sufficient attention mass.

the figure shows substantial variability across samples: the same budget can yield near-complete attention recovery in some cases while severely underestimating attention mass in others. This reflects highly non-uniform attention distributions across inputs and demonstrates that no single fixed token budget can reliably satisfy top-p constraints. Consequently, token-level top-p methods must adopt conservative, over-provisioned budgets to avoid failure, which directly hurts their efficiency advantages.

Second, because estimation operates at the token level, the cost of top-p selection scales linearly with the number of tokens considered. Figure 4 shows that attention score estimation via SpGEMV and subsequent top-p selection together account for a large fraction of the total decoding time. This overhead persists regardless of how aggressively tokens are pruned afterward, since both stages operate at the token level and scale linearly with context length. As a result, even though Twilight reduces the cost of the final sparse attention computation, the high estimation overhead fundamentally limits end-to-end speedups. This observation motivates reducing the cost of top-p estimation itself, rather than relying solely on pruning after selection.

On the other hand, cluster-based sparse attention methods (Chen et al., 2025) reduce sparse attention cost by operating on cluster-level representations. While efficient, both cluster selection and token-level computation in these methods rely on fixed cluster or token budgets. Consequently, they lack explicit control over preserved attention mass and cannot provide accuracy guarantees aligned with top-p objectives.

Together, these limitations expose a key gap in the design space: existing methods either support top-p selection at high estimation cost or achieve efficiency by reverting to fixed-budget top-k behavior. Bridging this gap requires rethinking top-p sparse attention as an end-to-end problem that jointly considers estimation, selection, and sparse

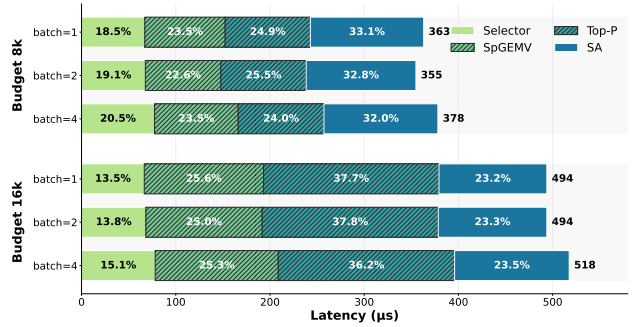


Figure 4. Latency Breakdown of Token-Level Top-p Sparse Attention. Shaded bars indicate Top-p estimation overhead. Token-level attention score estimation (SpGEMV) and Top-p selection account for a substantial fraction of total latency, indicating that top-p estimation overhead dominates performance even before sparse attention (SA) is applied.

computation, motivating a hierarchical approach that aligns probability-based pruning with the structure of sparse attention systems.

## 4. Double-P Sparse Attention

In this section, we present Double-P, a hierarchical top-p sparse attention framework designed to jointly optimize top-p estimation accuracy, selection overhead, and sparse attention cost, shown in Figure 5. Double-P exploits the hierarchical structure of modern sparse attention systems by first estimating attention mass at the cluster level and then adaptively refining token-level computation through a second top-p stage. This design enables accurate, probability-driven pruning while avoiding fixed token budgets.

### 4.1. Prefilling

During the prefill stage, the input context is processed once to construct the key-value (KV) cache, where keys and values are stored as matrices  $\mathbf{K}, \mathbf{V} \in \mathbb{R}^{N \times d}$ , with  $N$  denoting the context length and  $d$  the attention head dimension. To enable coarse-grained attention estimation, we partition the KV cache into clusters by applying k-means clustering (Hartigan & Wong, 1979) over the key vectors  $\mathbf{K}$ . This groups tokens with similar key representations into semantically coherent clusters.

For each cluster  $i$  with token set  $\mathcal{T}_i$ , cluster centroid  $\mathbf{C}_i$  size  $s_i = |\mathcal{T}_i|$ , we aggregate token values into a single cluster-level representation by summing over tokens,

$$\mathbf{V}_i^\Sigma = \sum_{j \in \mathcal{T}_i} \mathbf{v}_{ij}, \quad \bar{\mathbf{V}}_i = \frac{1}{s_i} \mathbf{V}_i^\Sigma, \quad (2)$$

where  $\mathbf{v}_{ij}$  is the  $j$ -th value vector in  $i$ -th cluster,  $\mathbf{V}_i^\Sigma$  denotes the sum of values and  $\bar{\mathbf{V}}_i$  its normalized average.

Together, the cluster centroid  $\mathbf{C}_i$ , size  $s_i$ , and value aggregates provide a compact and efficient summary of the KV

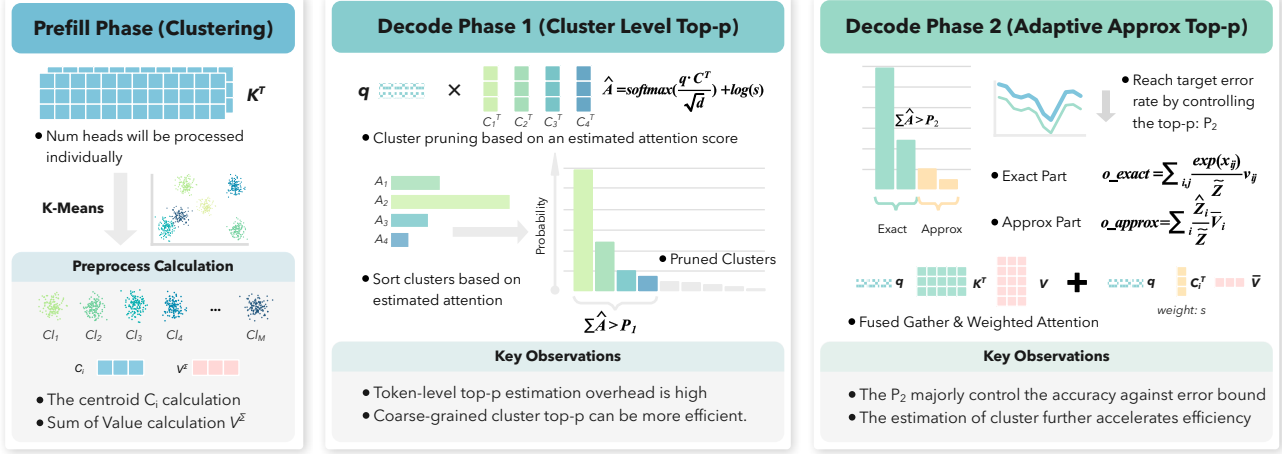


**Figure 5. Double-P framework overview.** Double-P performs hierarchical top-p sparse attention by first estimating attention mass at the cluster level using size-weighted centroids, then adaptively refining token-level computation through a second top-p stage. Exact token attention and centroid-based approximations are combined to achieve high accuracy with low estimation and sparse attention cost.

cache. These representations enable low-cost estimation of attention mass at the cluster level and support mixed-granularity attention computation in later stages of Double-P.

#### 4.2. Stage 1: Cluster-Level Attention Score Estimation

During decoding stage, given a query vector  $q \in \mathbb{R}^{1 \times d}$ , consider a cluster  $i$  of tokens  $\mathcal{T}_i$  with centroid  $C_i \in \mathbb{R}^{1 \times d}$  and size  $s_i$ . We first define the corresponding attention logits as

$$x_{ij} = \frac{q \mathbf{k}_{ij}^\top}{\sqrt{d}}, \quad \bar{x}_i = \frac{q C_i^\top}{\sqrt{d}}. \quad (3)$$

where  $\mathbf{k}_{ij}$  is the  $j$ -th key vector in  $i$ -th cluster,  $x_{ij}$  denotes the exact token-level attention logit and  $\bar{x}_i$  is its centroid-based approximation. The exact cluster mass is

$$Z_i = \sum_{j \in \mathcal{T}_i} \exp(x_{ij}). \quad (4)$$

Computing  $Z_i$  exactly requires evaluating all token-level logits, which is expensive. Instead, we approximate the cluster mass using the centroid logit scaled by the cluster size:

$$\hat{Z}_i = s_i \exp(\bar{x}_i), \quad \log \hat{Z}_i = \bar{x}_i + \log s_i. \quad (5)$$

Let  $\mathbf{C} \in \mathbb{R}^{K \times d}$  denote the matrix of all cluster centroids, with rows  $C_i$ , and let  $s \in \mathbb{R}^K$  be the vector of cluster sizes. Normalizing these approximate masses yields an estimated cluster-level attention distribution,

$$\hat{\mathbf{A}} = \frac{\hat{\mathbf{Z}}}{\sum_\ell \hat{Z}_\ell} = \text{softmax}\left(\frac{q \mathbf{C}^\top}{\sqrt{d}} + \log s\right), \quad (6)$$

where  $\hat{\mathbf{A}}$  serves as an approximation of the attention mass assigned to the clusters.

Compared to token-level estimation, this formulation provides a low-cost yet informative estimate of how attention is distributed across clusters. We then apply a Top-P selection over clusters to identify the minimal set whose cumulative attention mass exceeds a target threshold  $p_1$

$$\mathcal{C}_p = \left\{ i \mid \sum_{i \in \mathcal{C}_p} \hat{A}_i \geq p \right\}, \quad (7)$$

with clusters sorted by  $\hat{A}_i$  in descending order.

#### 4.3. Stage 2: Adaptive Token Budget Allocation for Sparse Attention

While the first-stage cluster-level Top-P provides a coarse estimate of attention mass, computing exact token-level attention for all selected clusters remains unnecessary and inefficient. Figure 6 visualizes the absolute attention error introduced by replacing token-level attention with cluster-centroid estimates across layers and decoding steps. The error is strongly long-tailed: a small number of clusters contribute the majority of approximation error, while most clusters have negligible impact. Besides, the error distribution varies significantly across layers and decoding steps.

Figure 7 further quantifies this observation by showing the minimum number of clusters that must be computed with exact attention to satisfy a fixed error bound. The required number fluctuates widely across layers and decoding steps, indicating that enforcing a fixed cluster or token budget would either waste computation or violate accuracy guarantees.

To address this challenge, we introduce an *adaptive token budget allocation* mechanism for sparse attention based on a

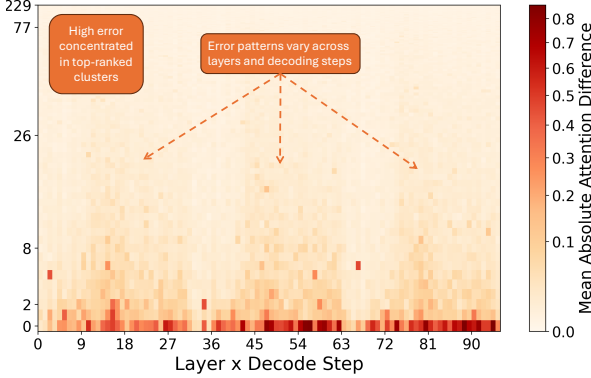


Figure 6. Heatmap of absolute error between exact token-level attention and cluster-centroid-based approximation, indexed by cluster rank. High approximation error is concentrated in a small number of top-ranked clusters, while the error distribution varies significantly across layers and decoding steps.

second Top-P stage. Rather than assigning a fixed token budget, this stage refines computation by allocating token-level attention in proportion to each cluster’s estimated contribution to the overall attention mass. Clusters with higher impact are assigned exact token-level computation, while clusters with lower impact are approximated using centroid-based summaries. The emphasized curve shown in Figure 7 corresponds to the clusters selected by the second-stage top-p in Double-P, which closely matches the minimum required clusters given a certain error threshold. This result shows that the second top-p effectively allocates exact computation only where necessary, achieving near-minimal cost while maintaining bounded attention error.

After the second top-p selection, we partition the clusters into two disjoint sets: clusters that receive exact token-level attention and clusters whose contributions are approximated. Let  $\mathcal{C}_{\text{exact}}$  denote the set of clusters assigned to exact computation, and  $\mathcal{C}_{\text{approx}}$  denote the remaining clusters.

To combine exact and approximate contributions in a unified manner, we normalize both using a shared attention mass,

$$\tilde{Z} = \sum_{i \in \mathcal{C}_{\text{exact}}} \sum_{j \in \mathcal{T}_i} \exp(x_{ij}) + \sum_{i \in \mathcal{C}_{\text{approx}}} \hat{Z}_i. \quad (8)$$

The final attention output is then computed as a mixture of exact and approximate contributions,

$$\mathbf{o}(\mathbf{q}) = \sum_{i \in \mathcal{C}_{\text{exact}}} \sum_{j \in \mathcal{T}_i} \frac{\exp(x_{ij})}{\tilde{Z}} \mathbf{v}_{ij} + \sum_{i \in \mathcal{C}_{\text{approx}}} \frac{\hat{Z}_i}{\tilde{Z}} \bar{\mathbf{V}}_i, \quad (9)$$

where exact tokens contribute through their full attention weights, and approximate clusters contribute proportionally to their estimated attention mass.

#### 4.4. Efficient kernel implementation

We design efficient GPU kernel implementations that minimizes selection overhead and maximizes data locality during

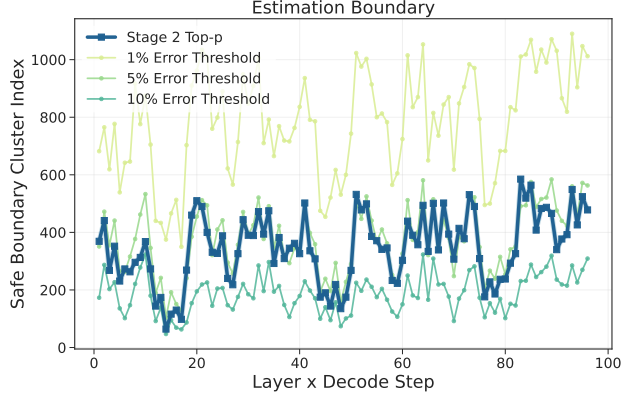


Figure 7. Adaptive cluster selection for bounded attention error. The minimum number of clusters required to satisfy a given error threshold varies significantly across layers and decoding steps. The **bold** line shows the number of clusters selected by the second-stage Top-P in Double-P, which closely tracks the minimum required clusters, demonstrating near-optimal adaptive allocation.

sparse attention computation.

**Efficient Top-p.** Both stages of Double-P rely on Top-P selection over attention scores that are already sorted. We implement a custom Top-P kernel that operates directly on sorted tensors, performing prefix-sum accumulation and early stopping to identify the minimal set of elements whose cumulative probability exceeds the target threshold.

**Efficient Token & Cluster Gathering.** After second Top-P selection, we fuse gathering selected tokens and cluster centroids into one kernel, and copy them into a contiguous memory buffer. This fusion step enables coalesced reads for subsequent attention computation.

**Efficient Sparse Attention.** We compute sparse attention using a weighted variant of FlashAttention over the fused buffers, introduced by RetroInfer (Chen et al., 2025). Exact tokens and approximate cluster summaries are processed uniformly within the same attention kernel. This design avoids separate kernels for exact and approximate attention.

## 5. Evaluation

We evaluate Double-P from both accuracy and efficiency perspectives to assess its effectiveness for long-context inference. Our experiments focus on (i) downstream task accuracy, and (ii) end-to-end decoding latency with detailed breakdowns of estimation and sparse attention cost. We compare against state-of-the-art baselines across multiple benchmarks, and context lengths to demonstrate robustness and practical accuracy efficiency gains.

### 5.1. Experimental Setup

**Hardware and system configuration.** All experiments are conducted on a single-node GPU server equipped with one

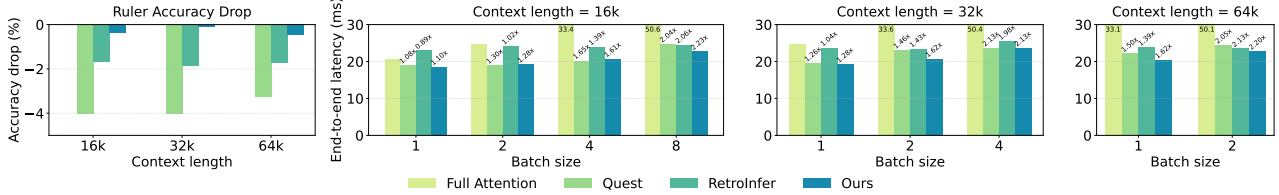


Figure 8. Accuracy drop and end-to-end decoding latency on RULER. Double-P achieves **near-zero** accuracy drop compared with full attention while consistently delivering faster inference.

NVIDIA H100 PCIe GPU (80GB memory) and an Intel(R) Xeon(R) Gold 5416S CPU, using CUDA 12.8 and PyTorch 2.8.

**Models.** We evaluate Double-P on the representative open-source long-context LLM: LLaMA3.1-8B (Grattafiori et al., 2024), with context lengths up to 128K tokens. It has 32 layers and 32 heads, adopts group query attention (GQA) with group size 4.

**Baselines.** We compare Double-P against representative sparse attention baselines covering both page-level and cluster-based designs. For fair comparison, all methods preserve sink tokens (4 tokens) and sliding-window tokens (64 tokens) at every layer (Xiao et al., 2023), while sparse attention is applied only to the remaining middle tokens. (1) **Quest** (Tang et al., 2024b) is a page-level method that selects top-k pages based on key bounds; we follow the default page size 16 and retrieve 25% of the tokens. (2) **RetroInfer** (Chen et al., 2025) is a cluster-based method that retrieves a fixed number of top-k clusters and performs sparse attention over tokens and cluster centroids; we use the cluster configurations and retrieval budgets suggested by the authors. (3) **Twilight** (Lin et al., 2025) is a token-level top-p sparse attention method that performs select-then-prune using approximate token-level attention estimation under a fixed selection budget; we use the recommended 25% token budget from the original paper on Quest.

**Benchmarks.** We evaluate accuracy on two established long-context benchmarks. (1) **RULER** (Hsieh et al., 2024) is a comprehensive benchmark consisting of 13 tasks, with context lengths ranging from 4K to 128K tokens. (2) **LongBench** (Bai et al., 2024) focuses on realistic long-context applications and comprises six major task categories with 21 individual tasks. The average input length of most tasks ranges from 5K to 15K tokens.

## 5.2. Accuracy

**Accuracy on RULER.** Table 2 reports average RULER accuracy for LLaMA-3.1-8B across context lengths. Double-P consistently achieves the highest accuracy among sparse attention methods, improving over the strongest baseline by **+1.31**, **+1.79**, and **+0.78** absolute points at 16K, 32K, and

Table 2. Accuracy comparison on Ruler and LongBench for LLaMA3.1-8B.

Method	16k	32k	64k	Avg.	LongBench
LLaMA-3.1-8B	93.25	90.00	85.36	89.54	39.33
Quest	89.24	85.95	83.61	86.27	38.76
RetroInfer	91.56	88.12	83.77	87.82	39.03
Quest + Twi	86.73	86.50	81.87	85.03	38.97
<b>Double-P (Ours)</b>	<b>92.87</b>	<b>89.91</b>	<b>84.55</b>	<b>89.08</b>	<b>39.06</b>
	<b>+1.31</b>	<b>+1.79</b>	<b>+0.78</b>	<b>+1.26</b>	<b>+0.03</b>

64K context lengths, respectively. On average, Double-P yields a **+1.26** point gain and achieves **near-zero accuracy drop** compared with full attention. These results demonstrate that Double-P preserves attention mass more reliably than prior methods, translating directly into higher accuracy under long-context inference.

**Accuracy on LongBench.** Table 2 reports performance on LongBench. Double-P achieves the highest accuracy among all sparse attention methods and remains within a near-zero gap to full attention. Double-P maintains strong generalization across heterogeneous LongBench tasks, demonstrating that its probability-driven selection strategy preserves attention quality beyond synthetic benchmarks.

We report the full per-task accuracy results in the appendix.

## 5.3. Efficiency

We evaluate the efficiency of Double-P and other baselines with different context lengths and batch sizes. We use Llama-3.1-8B and NIAH to measure both attention latency breakdown and end-to-end decoding latency.

**Attention latency.** Figure 9 shows the breakdown of attention computation across sparse attention methods, where **shaded bars indicate top-p estimation overhead**. In existing top-p approaches, token-level estimation dominates attention latency, accounting for **over 60%** of the total cost. Double-P largely eliminates this overhead by replacing token-level estimation with efficient cluster-level approximation. In addition, its **adaptive token budget allocation** significantly reduces the cost of the final sparse attention step by avoiding unnecessary token-level computation on low-impact clusters. Together, these effects enable Double-

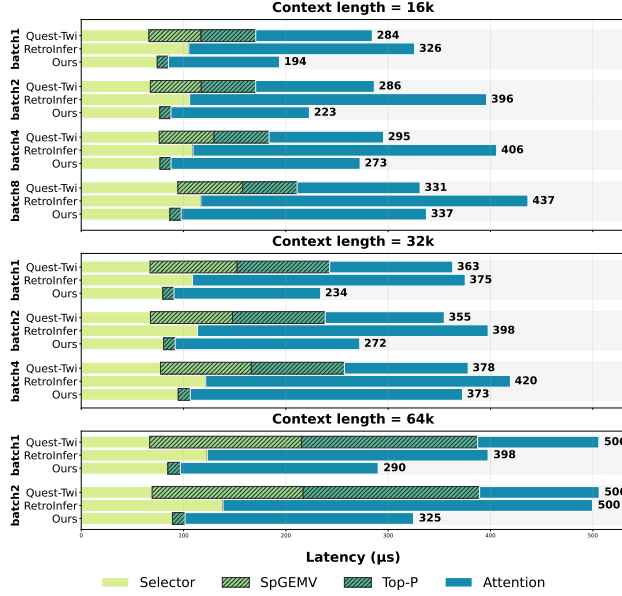


**Figure 9. Attention latency breakdown.** Shaded bars indicate top-p estimation overhead. Double-P minimizes this cost and achieves significant attention-level speedups compared to prior sparse attention methods.

P to achieve up to **1.74**× and **1.78**× attention-level speedup over Quest-Twilight and RetroInfer, respectively.

**End-to-end decoding latency.** Figure 8 reports the end-to-end decoding latency per output token across sparse attention methods, together with the corresponding accuracy drop relative to full attention. Double-P achieves up to **1.11**× and **1.26**× speedup over Quest and RetroInfer, respectively, while maintaining a **near-zero accuracy drop** compared with full attention. Moreover, Double-P outperforms full attention by **up to 2.23**×, demonstrating that its algorithmic efficiency translates directly into practical decoding speedups without sacrificing accuracy.

#### 5.4. Ablation Study

Figure 10 analyzes the sensitivity of Double-P to the two top-p thresholds controlling attention mass preservation at the cluster level ( $p_1$ ) and token-level refinement ( $p_2$ ). Varying these parameters reveals a clear accuracy–efficiency trade-off: larger  $p_1$  and  $p_2$  retain a greater fraction of attention mass and improve accuracy, while smaller values reduce computation and yield higher efficiency. In practice, we select  $(p_1, p_2) = (0.95, 0.7)$  for LLaMA-3.1-8B, which provides a balanced trade-off between accuracy and speed.

We further evaluate Double-P on the Qwen-3-8B model (Yang et al., 2025a), with  $(p_1, p_2) = (0.99, 0.8)$ . The corresponding accuracy results on RULER and LongBench are reported in Table 3.

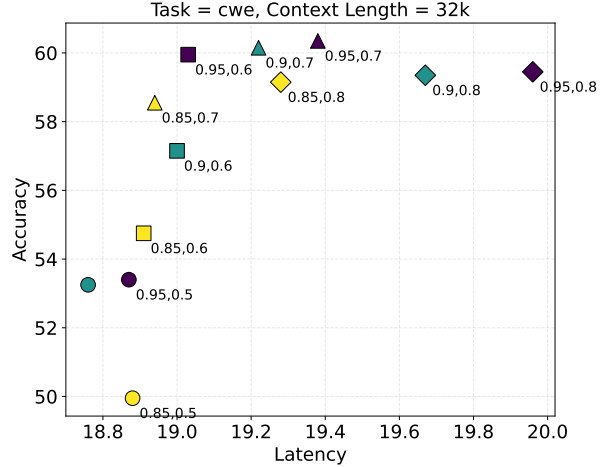


**Figure 10.** Accuracy and latency of different Double-P configurations tested on Ruler 32k cwe task.

**Table 3.** Accuracy comparison on Ruler and LongBench for Qwen3-8B.

Method	16k	32k	64k	Avg.	LongBench
Qwen3-8B	91.25	90.59	80.40	87.41	35.82
Quest	77.12	79.80	60.12	72.35	35.52
RetroInfer	91.16	90.65	80.09	87.3	35.63
Quest + Twi	76.69	79.50	58.59	71.59	35.26
<b>Double-P (Ours)</b>	91.02	90.36	79.26	86.88	35.78

## 6. Conclusion

This paper proposes **Double-P**, a hierarchical top-p sparse attention framework for efficient long-context LLM inference. By jointly optimizing attention mass estimation, candidate selection, and sparse attention, Double-P aligns probability-based pruning with the hierarchical structure of sparse attention systems, eliminating fixed-budget constraints and enabling adaptive allocation of token-level computation across decoding steps. As a result, Double-P preserves top-p attention guarantees and consistently achieves higher accuracy than prior sparse attention methods, remaining within a near-zero gap to full attention. At the same time, Double-P delivers substantial efficiency improvements, achieving up to 1.78× attention-level speedup over token-level top-p methods and up to 1.26× end-to-end decoding speedup over strong sparse attention baselines, while accelerating inference by up to 2.23× compared to full attention. These findings demonstrate that effective top-p sparse attention requires adaptive, probability-driven computation across multiple levels of abstraction, and position Double-P as a principled and scalable foundation for future sparse attention designs in long-context language models.

## Acknowledgements

This paper is supported in part by SRC JUMP 2.0 Center for Processing with Intelligent Storage and Memory (PRISM) and Center for Machine-Integrated Computing and Security (MICS).

## Impact Statement

This paper presents a new sparse attention framework aimed at improving the efficiency and accuracy of long-context inference in large language models. By reducing computational and memory overhead while preserving attention quality, this work contributes to more scalable and accessible deployment of LLMs in practical applications such as document understanding, retrieval, and reasoning over long inputs.

The techniques introduced in this paper are purely algorithmic and system-level improvements to existing attention mechanisms and do not introduce new capabilities that fundamentally alter the intended use of language models. As such, we do not foresee direct negative societal or ethical consequences arising uniquely from this work beyond those already associated with large language models more broadly.

## References

Appalaraju, S., Jasani, B., Kota, B. U., Xie, Y., and Manmatha, R. Docformer: End-to-end transformer for document understanding. In *Proceedings of the IEEE/CVF international conference on computer vision*, pp. 993–1003, 2021.

Bai, Y., Lv, X., Zhang, J., Lyu, H., Tang, J., Huang, Z., Du, Z., Liu, X., Zeng, A., Hou, L., et al. Longbench: A bilingual, multitask benchmark for long context understanding. In *Proceedings of the 62nd annual meeting of the association for computational linguistics (volume 1: Long papers)*, pp. 3119–3137, 2024.

Chen, Y., Zhang, J., Lu, B., Zhang, Q., Zhang, C., Luo, J., Liu, D., Jiang, H., Chen, Q., Liu, J., et al. Retroinfer: A vector-storage approach for scalable long-context llm inference. *arXiv preprint arXiv:2505.02922*, 2025.

Chen, Z., Sadhukhan, R., Ye, Z., Zhou, Y., Zhang, J., Nolte, N., Tian, Y., Douze, M., Bottou, L., Jia, Z., et al. Mag-icpig: Lsh sampling for efficient llm generation. *arXiv preprint arXiv:2410.16179*, 2024.

Fan, W., Ding, Y., Ning, L., Wang, S., Li, H., Yin, D., Chua, T.-S., and Li, Q. A survey on rag meeting llms: Towards retrieval-augmented large language models. In *Proceedings of the 30th ACM SIGKDD conference on knowledge discovery and data mining*, pp. 6491–6501, 2024.

Feng, Y., Lv, J., Cao, Y., Xie, X., and Zhou, S. K. Adakv: Optimizing kv cache eviction by adaptive budget allocation for efficient llm inference. *arXiv preprint arXiv:2407.11550*, 2024.

Frantar, E., Ashkboos, S., Hoefer, T., and Alistarh, D. Gptq: Accurate post-training quantization for generative pre-trained transformers. *arXiv preprint arXiv:2210.17323*, 2022.

Gao, Y., Zeng, Z., Du, D., Cao, S., Zhou, P., Qi, J., Lai, J., So, H. K.-H., Cao, T., Yang, F., et al. Seerattention: Learning intrinsic sparse attention in your llms. *arXiv preprint arXiv:2410.13276*, 2024.

Grattafiori, A., Dubey, A., Jauhri, A., Pandey, A., Kadian, A., Al-Dahle, A., Letman, A., Mathur, A., Schelten, A., Vaughan, A., et al. The llama 3 herd of models. *arXiv preprint arXiv:2407.21783*, 2024.

Gu, A. and Dao, T. Mamba: Linear-time sequence modeling with selective state spaces. In *First conference on language modeling*, 2024.

Hartigan, J. A. and Wong, M. A. Algorithm as 136: A k-means clustering algorithm. *Journal of the royal statistical society. series c (applied statistics)*, 28(1):100–108, 1979.

Hooper, C., Kim, S., Mohammadzadeh, H., Mahoney, M. W., Shao, Y. S., Keutzer, K., and Gholami, A. Kvquant: Towards 10 million context length llm inference with kv cache quantization. *Advances in Neural Information Processing Systems*, 37:1270–1303, 2024.

Hsieh, C.-P., Sun, S., Kriman, S., Acharya, S., Rekesh, D., Jia, F., Zhang, Y., and Ginsburg, B. Ruler: What’s the real context size of your long-context language models? *arXiv preprint arXiv:2404.06654*, 2024.

Jiang, H., Li, Y., Zhang, C., Wu, Q., Luo, X., Ahn, S., Han, Z., Abdi, A. H., Li, D., Lin, C.-Y., et al. Minference 1.0: Accelerating pre-filling for long-context llms via dynamic sparse attention. *Advances in Neural Information Processing Systems*, 37:52481–52515, 2024.

Jin, B., Yoon, J., Han, J., and Arik, S. O. Long-context llms meet rag: Overcoming challenges for long inputs in rag. *arXiv preprint arXiv:2410.05983*, 2024.

Jones, D., Park, J., Morse, M. J., Lee, M., Langston, M. H., and Lott, C. Quoka: Query-oriented kv selection for efficient llm prefill. *ICLR 2026*, 2026.

Kang, H., Zhang, Q., Kundu, S., Jeong, G., Liu, Z., Krishna, T., and Zhao, T. Gear: An efficient kv cache compression recipe for near-lossless generative inference of llm. *arXiv preprint arXiv:2403.05527*, 2024.

Katharopoulos, A., Vyas, A., Pappas, N., and Fleuret, F. Transformers are rnns: Fast autoregressive transformers with linear attention. In *International conference on machine learning*, pp. 5156–5165. PMLR, 2020.

Kwon, W., Li, Z., Zhuang, S., Sheng, Y., Zheng, L., Yu, C. H., Gonzalez, J., Zhang, H., and Stoica, I. Efficient memory management for large language model serving with pagedattention. In *Proceedings of the 29th symposium on operating systems principles*, pp. 611–626, 2023.

Li, Y., Huang, Y., Yang, B., Venkitesh, B., Locatelli, A., Ye, H., Cai, T., Lewis, P., and Chen, D. Snapkv: Llm knows what you are looking for before generation. *Advances in Neural Information Processing Systems*, 37:22947–22970, 2024.

Lin, C., Tang, J., Yang, S., Wang, H., Tang, T., Tian, B., Stoica, I., Han, S., and Gao, M. Twilight: Adaptive attention sparsity with hierarchical top- $p$  pruning. *arXiv preprint arXiv:2502.02770*, 2025.

Lin, J., Tang, J., Tang, H., Yang, S., Chen, W.-M., Wang, W.-C., Xiao, G., Dang, X., Gan, C., and Han, S. Awq: Activation-aware weight quantization for on-device llm compression and acceleration. *Proceedings of machine learning and systems*, 6:87–100, 2024.

Liu, A., Mei, A., Lin, B., Xue, B., Wang, B., Xu, B., Wu, B., Zhang, B., Lin, C., Dong, C., et al. Deepseek-v3. 2: Pushing the frontier of open large language models. *arXiv preprint arXiv:2512.02556*, 2025a.

Liu, D., Chen, M., Lu, B., Jiang, H., Han, Z., Zhang, Q., Chen, Q., Zhang, C., Ding, B., Zhang, K., et al. Retrievalattention: Accelerating long-context llm inference via vector retrieval. *arXiv preprint arXiv:2409.10516*, 2024.

Liu, G., Li, C., Zhao, J., Zhang, C., and Guo, M. Clusterkv: Manipulating llm kv cache in semantic space for recallable compression. In *2025 62nd ACM/IEEE Design Automation Conference (DAC)*, pp. 1–7. IEEE, 2025b.

Liu, Z., Luo, X., Guo, J., Ni, W., Zhou, Y., Guan, Y., Guo, C., Cui, W., Feng, Y., Guo, M., et al. Vq-llm: High-performance code generation for vector quantization augmented llm inference. In *2025 IEEE International Symposium on High Performance Computer Architecture (HPCA)*, pp. 1496–1509. IEEE, 2025c.

Liu, Z., Ni, W., Leng, J., Feng, Y., Guo, C., Chen, Q., Li, C., Guo, M., Ma, Y., Zhang, F., et al. Juno++: Optimizing anns and enabling efficient sparse attention in llm via ray tracing core. *ACM Transactions on Architecture and Code Optimization*, 22(4):1–25, 2025d.

Lu, E., Jiang, Z., Liu, J., Du, Y., Jiang, T., Hong, C., Liu, S., He, W., Yuan, E., Wang, Y., et al. Moba: Mixture of block attention for long-context llms. *arXiv preprint arXiv:2502.13189*, 2025.

Luo, C., Shen, Y., Zhu, Z., Zheng, Q., Yu, Z., and Yao, C. Layoutllm: Layout instruction tuning with large language models for document understanding. In *Proceedings of the IEEE/CVF conference on computer vision and pattern recognition*, pp. 15630–15640, 2024.

Tang, H., Lin, Y., Lin, J., Han, Q., Hong, S., Yao, Y., and Wang, G. Razorattention: Efficient kv cache compression through retrieval heads. *arXiv preprint arXiv:2407.15891*, 2024a.

Tang, J., Zhao, Y., Zhu, K., Xiao, G., Kasikci, B., and Han, S. Quest: Query-aware sparsity for efficient long-context llm inference. *arXiv preprint arXiv:2406.10774*, 2024b.

Team, G., Anil, R., Borgeaud, S., Alayrac, J.-B., Yu, J., Soricut, R., Schalkwyk, J., Dai, A. M., Hauth, A., Millican, K., et al. Gemini: a family of highly capable multimodal models. *arXiv preprint arXiv:2312.11805*, 2023.

Tseng, A., Chee, J., Sun, Q., Kuleshov, V., and De Sa, C. Quip#: Even better llm quantization with hadamard incoherence and lattice codebooks. *arXiv preprint arXiv:2402.04396*, 2024.

Van Baalen, M., Kuzmin, A., Koryakovskiy, I., Nagel, M., Couperus, P., Bastoul, C., Mahurin, E., Blankevoort, T., and Whatmough, P. Gptvq: The blessing of dimensionality for llm quantization. *arXiv preprint arXiv:2402.15319*, 2024.

Vaswani, A., Shazeer, N., Parmar, N., Uszkoreit, J., Jones, L., Gomez, A. N., Kaiser, Ł., and Polosukhin, I. Attention is all you need. *Advances in neural information processing systems*, 30, 2017.

Xiao, G., Tian, Y., Chen, B., Han, S., and Lewis, M. Efficient streaming language models with attention sinks. *arXiv preprint arXiv:2309.17453*, 2023.

Xiao, G., Tang, J., Zuo, J., Guo, J., Yang, S., Tang, H., Fu, Y., and Han, S. Duoattention: Efficient long-context llm inference with retrieval and streaming heads. *arXiv preprint arXiv:2410.10819*, 2024.

Xu, R., Xiao, G., Huang, H., Guo, J., and Han, S. Xattention: Block sparse attention with antidiagonal scoring. *arXiv preprint arXiv:2503.16428*, 2025.

Yang, A., Li, A., Yang, B., Zhang, B., Hui, B., Zheng, B., Yu, B., Gao, C., Huang, C., Lv, C., et al. Qwen3 technical report. *arXiv preprint arXiv:2505.09388*, 2025a.

Yang, A., Yu, B., Li, C., Liu, D., Huang, F., Huang, H., Jiang, J., Tu, J., Zhang, J., Zhou, J., et al. Qwen2. 5-1m technical report. *arXiv preprint arXiv:2501.15383*, 2025b.

Yang, S., Guo, J., Tang, H., Hu, Q., Xiao, G., Tang, J., Lin, Y., Liu, Z., Lu, Y., and Han, S. Lserve: Efficient long-sequence llm serving with unified sparse attention. *arXiv preprint arXiv:2502.14866*, 2025c.

Yuan, J., Gao, H., Dai, D., Luo, J., Zhao, L., Zhang, Z., Xie, Z., Wei, Y., Wang, L., Xiao, Z., et al. Native sparse attention: Hardware-aligned and natively trainable sparse attention. In *Proceedings of the 63rd Annual Meeting of the Association for Computational Linguistics (Volume 1: Long Papers)*, pp. 23078–23097, 2025.

Yue, Y., Yuan, Z., Duanmu, H., Zhou, S., Wu, J., and Nie, L. Wkvquant: Quantizing weight and key/value cache for large language models gains more. *arXiv preprint arXiv:2402.12065*, 2024.

Zhang, H., Ji, X., Chen, Y., Fu, F., Miao, X., Nie, X., Chen, W., and Cui, B. Pqcache: Product quantization-based kvcache for long context llm inference. *Proceedings of the ACM on Management of Data*, 3(3):1–30, 2025a.

Zhang, J., Xiang, C., Huang, H., Wei, J., Xi, H., Zhu, J., and Chen, J. Spargeattn: Accurate sparse attention accelerating any model inference. *arXiv preprint arXiv:2502.18137*, 2025b.

Zhang, Z., Sheng, Y., Zhou, T., Chen, T., Zheng, L., Cai, R., Song, Z., Tian, Y., Ré, C., Barrett, C., et al. H2o: Heavy-hitter oracle for efficient generative inference of large language models. *Advances in Neural Information Processing Systems*, 36:34661–34710, 2023.

Zhu, K., Tang, T., Xu, Q., Gu, Y., Zeng, Z., Kadekodi, R., Zhao, L., Li, A., Krishnamurthy, A., and Kasikci, B. Tactic: Adaptive sparse attention with clustering and distribution fitting for long-context llms. *arXiv preprint arXiv:2502.12216*, 2025.

## A. Full Benchmark Results

### A.1. Ruler

Table 4. Ruler results across tasks for LLaMA-3.1-8B and Qwen3-8B, 16K context length.

Method	s1_niah	s2_niah	s3_niah	mk1_niah	mk2_niah	mk3_niah	mv_niah	mq_niah	vt	fwe	cwe	qa_1	qa_2	Avg.
LLaMA-3.1-8B	100.00	100.00	100.00	100.00	100.00	100.00	96.50	100.00	99.60	89.60	98.00	82.00	64.00	94.59
Quest	99.00	100.00	87.00	100.00	96.00	70.00	95.25	97.75	98.60	86.50	88.00	84.00	58.00	89.24
RetroInfer	100.00	99.50	99.50	100.00	98.50	96.50	95.62	99.88	99.90	82.40	87.00	76.00	55.50	91.56
Quest + Twi	99.00	100.00	80.50	96.00	95.50	69.50	94.62	96.50	98.80	81.70	86.33	74.50	54.50	86.73
<b>Ours</b>	100.00	100.00	100.00	100.00	99.5	98.00	97.00	99.75	99.50	92.90	88.67	78.00	54.00	92.87
Qwen3-8B	100.00	100.00	100.00	99.50	100.00	99.00	92.88	100.00	100.00	91.65	93.17	59.50	50.50	91.25
Quest	98.00	98.00	53.00	99.00	84.00	40.00	86.25	86.38	94.30	67.40	90.67	58.50	47.00	77.12
RetroInfer	100.00	100.00	100.00	99.50	100.00	99.00	93.88	100.00	100.00	92.20	92.50	59.00	49.00	91.16
Quest + Twi	99.00	98.50	52.50	98.50	83.50	36.50	86.88	86.25	92.70	66.20	90.00	61.00	45.50	76.69
<b>Ours</b>	100.00	100.00	99.50	99.00	100.00	99.00	92.88	99.88	99.70	92.60	92.67	59.00	49.00	91.02

Table 5. Ruler results across tasks for LLaMA-3.1-8B and Qwen3-8B, 32K context length.

Method	s1_niah	s2_niah	s3_niah	mk1_niah	mk2_niah	mk3_niah	mv_niah	mq_niah	vt	fwe	cwe	qa_1	qa_2	Avg.
LLaMA-3.1-8B	100.00	100.00	100.00	98.50	100.00	100.00	97.38	99.25	99.80	50.40	95.17	75.50	54.00	90.00
Quest	97.50	100.00	86.50	99.00	97.50	89.00	92.38	96.50	99.00	44.50	90.00	73.00	52.50	85.95
RetroInfer	100.00	100.00	100.00	98.00	99.50	98.50	95.38	98.75	99.20	37.20	90.50	76.00	52.50	88.12
Quest + Twi	99.00	98.50	90.00	99.50	99.00	88.50	90.12	95.88	99.60	47.05	90.83	73.50	53.00	86.50
<b>Ours</b>	100.00	100.00	100.00	99.50	99.00	98.50	97.12	99.50	99.20	60.35	91.17	72.50	52.00	89.91
Qwen3-8B	100.00	100.00	100.00	99.00	97.50	96.50	99.00	99.50	99.80	80.65	95.17	60.50	50.00	90.59
Quest	100.00	100.00	72.50	99.50	89.00	43.50	93.12	86.62	92.60	60.85	90.17	62.00	47.50	79.80
RetroInfer	100.00	100.00	100.00	99.50	97.50	97.50	99.25	99.12	99.80	79.90	94.83	60.00	51.00	90.65
Quest + Twi	100.00	99.00	72.00	99.00	90.50	42.50	92.88	84.00	91.00	61.35	89.33	62.50	49.50	79.50
<b>Ours</b>	100.00	99.50	99.50	99.00	97.50	95.50	99.00	99.50	99.40	81.75	95.00	59.00	50.00	90.36

Table 6. Ruler results across tasks for LLaMA-3.1-8B and Qwen3-8B, 64K context length.

Method	s1_niah	s2_niah	s3_niah	mk1_niah	mk2_niah	mk3_niah	mv_niah	mq_niah	vt	fwe	cwe	qa_1	qa_2	Avg.
LLaMA-3.1-8B	100.00	100.00	100.00	100.00	99.00	96.50	98.38	99.75	98.70	9.50	86.33	72.50	49.00	85.36
Quest	100.00	99.50	93.50	96.50	98.00	90.50	98.39	98.62	95.75	9.95	85.17	73.00	48.00	83.61
RetroInfer	100.00	100.00	100.00	100.00	96.50	90.50	97.50	99.75	98.10	5.05	79.67	72.50	49.50	83.77
Quest + Twi	100.00	99.50	93.00	96.00	95.50	71.50	99.25	96.25	96.70	11.10	85.00	72.50	48.00	81.87
<b>Ours</b>	100.00	100.00	100.00	100.00	98.00	92.50	97.62	99.75	96.90	13.75	79.67	72.50	48.50	84.55
Qwen3-8B	100.00	100.00	100.00	90.50	76.50	31.00	95.50	97.25	99.70	68.20	78.50	66.50	41.50	80.40
Quest	99.50	69.50	35.50	69.50	58.50	3.00	78.75	71.50	85.30	35.95	78.00	59.50	37.00	60.12
RetroInfer	100.00	99.50	100.00	90.00	75.00	29.50	94.88	97.12	99.70	68.75	77.67	67.50	41.50	80.09
Quest + Twi	99.50	62.00	31.50	80.00	63.64	0.00	73.38	65.62	80.43	31.43	75.83	57.72	40.68	58.59
<b>Ours</b>	100.00	98.50	96.50	89.00	72.00	28.00	94.50	95.25	97.00	70.50	78.67	69.00	41.50	79.26

### A.2. LongBench

Table 7. LongBench results across tasks for LLaMA-3.1-8B and Qwen3-8B.

Method	2Wiki	Gov	Hotpot	Lcc	News	Field	Musi	Narr	Retriv	Qasper	Qnsum	Repo	Triv	Avg.
LLaMA-3.1-8B	16.16	34.38	16.82	63.16	26.74	27.64	11.72	31.96	97.73	13.18	23.23	57.03	91.48	39.33
Quest	16.27	34.51	16.69	63.22	26.86	27.27	11.94	33.77	96.58	12.94	23.75	50	90.03	38.76
RetroInfer	16.1	34.37	17.49	61.72	25.61	27.4	11.75	33.08	96.74	13.02	22.48	56.08	91.49	39.03
Quest + Twilight	16.38	34.05	16.72	63.55	26.82	26.92	11.54	31.43	95.78	12.85	23.25	56.23	91.02	38.96
<b>Ours</b>	16.18	34.93	17.1	62.85	26.78	27.36	11.47	32.07	96.22	12.67	22.66	56.17	91.32	39.06
Qwen3-8B	12.68	29.87	12.86	67.52	23.04	26.38	7.5	3.74	95.46	11.44	21.12	63.79	90.21	35.82
Quest	13.24	30.32	12.44	67.42	23.05	25.8	7.76	3.46	94.5	11.39	22.18	61.73	88.53	35.52
RetroInfer	12.08	29.91	12.73	67.5	22.69	26.04	7.89	3.62	94.25	11.43	20.53	64.35	90.21	35.63
Quest + Twilight	13.05	30.91	11.82	67.53	23.56	24.95	7.54	3.33	92.5	11.53	21.77	61.35	88.56	35.26
<b>Ours</b>	12.61	30.02	12.48	67.71	22.16	26.27	7.54	3.74	95.21	11.72	20.77	64.48	90.46	35.78